

# Metasomatism of cumulus magnesian olivine by iron-rich postcumulus liquids in the upper Critical Zone of the Bushveld Complex

ROGER N. SCOON

Department of Geology, Rhodes University, P.O. Box 94, Grahamstown 6140, South Africa

## Abstract

Hybrid olivine grains from locally concordant contact zones between bodies of iron-rich ultramafic pegmatite (postcumulate) and layered harzburgite (cumulate) are distinguished from cumulus olivine grains by petrographic features and compositional differences. The hybrid olivines, which in comparison with the cumulus crystals are Fe-Mn-rich and Mg-Ni-poor, represent an arrested stage of replacement and exhibit unusually high NiO/MgO ratios. These features are explained by a disequilibrium process of cation-for-cation exchange between crystals and silicate liquid i.e. magmatic metasomatism. Plots of cations across a contact zone give straight line relationships, a function of the extent to which the metasomatizing liquid infiltrated the cumulate layer. A plot of NiO against MgO enables a distinction to be made between metasomatic olivine and olivine that has fractionally crystallized from a tholeiitic magma. These metasomatic olivines all formed by the replacement of pre-existing cumulus olivine and no chemical evidence has been found to support the formation of olivine in iron-rich ultramafic pegmatite bodies by metasomatism of other phases.

KEYWORDS: Bushveld Complex, iron-rich ultramafic pegmatite, metasomatism, nickel, olivine, postcumulus, South Africa.

## Introduction

VILJOEN and Scoon (1985) classified discordant bodies of postcumulus, ultramafic rock in the Bushveld Complex, into three main categories: iron-rich ultramafic pegmatite, non-platiniferous magnesian dunite and platiniferous ultramafic pipes. Iron-rich ultramafic pegmatite is a broad name used to describe a suite of pegmatitic rocks, composed predominantly of iron-rich olivine, clinopyroxene and Fe-Ti oxides, that form veins, pod-like and pipe-like bodies (with diameters in excess of 1 km) which transgress the layered cumulates. Contacts between the discordant bodies of pegmatite and their host cumulates are usually sharp, if irregular. The formation of these rocks is not fully understood, although it is generally accepted that they are related to iron-rich, post-cumulus liquids (possibly in part intercumulus liquids) derived from within the crystallizing cumulate pile (Viljoen and Scoon, 1985). Most earlier publications (*inter alia*, Cameron and Desborough, 1964) concluded that the discordant pegmatite bodies in the Bushveld Complex resulted

from metasomatic replacement of pre-existing cumulates. However conclusive evidence of a metasomatic origin for these unusual rocks has not yet been assembled. Probably the most convincing evidence of metasomatism is found where pegmatite bodies form concordant contacts against chromitite layers, resulting in mixed Ti-magnetite-chromite-spinels (Cameron and Glover, 1973). In this paper I report compositional changes in olivine grains that occur in contact zones between such pegmatite bodies and harzburgite cumulates. These features may be compared with the chemical changes documented by Cameron and Glover (*op. cit.*) and both of these studies offer evidence of (magmatic) metasomatism, albeit on a very local scale.

This study is based on pegmatite bodies that occur in the upper Critical Zone of the layered sequence, at the Rustenburg Platinum Mines (RPM) Amandelbult Section mine, in the northern sector of the western Bushveld Complex. For a description of the cumulate sequence, the reader is referred to Viljoen *et al.* (1986) and Scoon and de Klerk (1987).

### Field relationships

Wagner, 1929, showed that iron-rich ultramafic pegmatite bodies selectively 'replace' (or, to avoid genetic implications, 'occur within') the more felsic cumulates in preference to mafic-ultramafic cumulates. Consequently, in parts of the layered sequence that consist of alternating layers of olivine-orthopyroxene cumulates and plagioclase cumulates, iron-rich ultramafic pegmatites occur as sheet-like, pseudo-layered bodies (see Fig. 6, Viljoen and Scoon, 1985).

In the upper Critical Zone between the UG-2 chromitite layer and the Merensky Reef at the Amandelbult Section mine occur a series of feldspathic harzburgite cumulates, known as the 'Pseudoreefs'. These ultramafic cumulates are rarely replaced by iron-rich ultramafic pegmatite, whereas adjacent and intercalated leuconorite and anorthosite layers commonly host such bodies. In the western part of the Amandelbult Section mine the Upper Pseudoreef is divided into three layers, the Upper Pseudoreefs A, B and C (Scoon and de

Klerk, 1987). Layers B and C, which correspond to the 'P2 marker' of Viljoen *et al.* (1986), are separated by a composite package, 1–1.2 m thick, of felsic cumulates (comprising leuconorite and anorthosite), colloquially referred to as the 'P2 middling'. The P2 middling may be selectively replaced by pegmatite, resulting in a locally concordant contact between the pegmatite body (above) and the Upper Pseudoreef B (below) [Fig. 1; case study (1)]. The Upper Pseudoreef B is underlain by a thin (1 cm) chromitite layer that is itself underlain by layers of anorthosite and leuconorite. The latter cumulates may be selectively replaced by pegmatite, resulting in a locally concordant contact between the pegmatite body (below) and the Upper Pseudoreef B (above) [Fig. 1; case study (2)].

### Petrography

The Upper Pseudoreef B is a coarse- to medium-grained feldspathic harzburgite that typically consists of 60–70% cumulus (magnesian) olivine, 0.5–1% cumulus chromite, 10–25% intercumulus

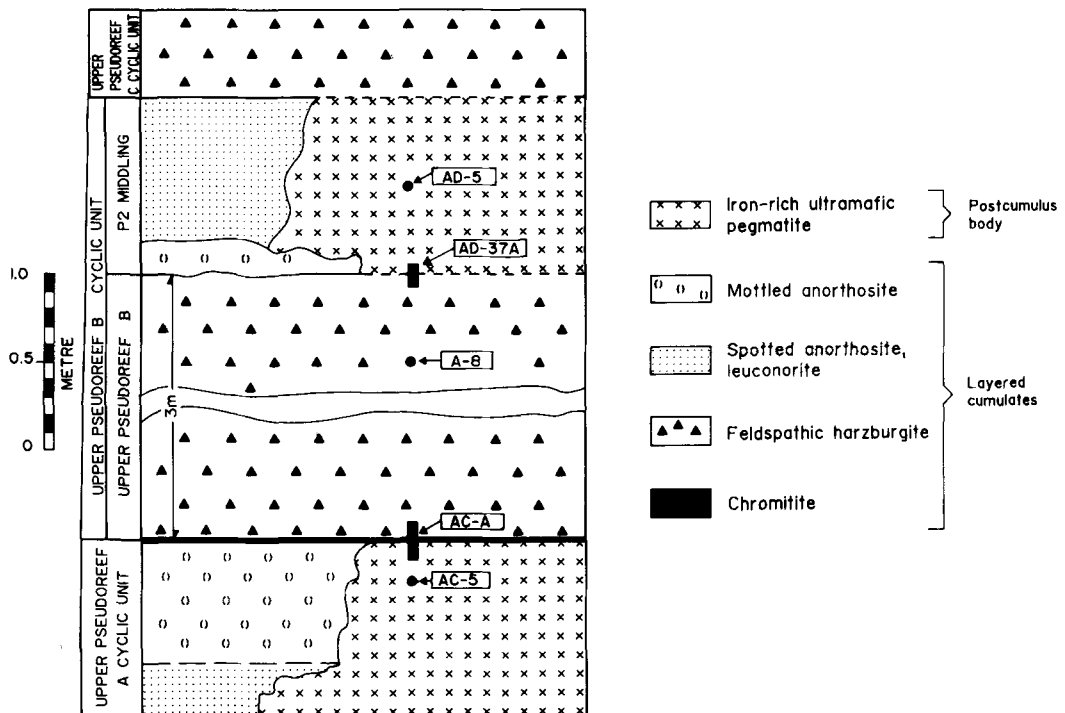


FIG. 1. Schematic strike section illustrating the concordant nature of iron-rich ultramafic pegmatite bodies occurring adjacent to the Upper Pseudoreef B. The pegmatite body replacing the 'P2 middling' forms case study (1)—samples AD-5 and AD-37A—and the pegmatite body replacing the felsic cumulates below the Upper Pseudoreef B forms case study (2)—samples AC-5 and AC-A.

orthopyroxene and 10-15% intercumulus plagioclase. Iron-rich ultramafic pegmatite in the upper Critical Zone consists of highly variable proportions of iron-rich olivine and clinopyroxene (these two minerals typically comprise over 85 modal %; in the I.U.G.S. classification these rocks include dunites, wehrlites and olivine clinopyroxenites), between 5 and 25% Fe-Ti oxides and accessory sulphides. Plagioclase is absent in iron-rich ultramafic pegmatite *sensu stricto*.

Petrographically the cumulus (magnesian) olivine and the pegmatitic (iron-rich) olivine can readily be distinguished. The cumulus olivine in the harzburgite layers occurs either as euhedral grains enclosed by poikilitic plagioclase, or as large, anhedral grains that are part of monomineralic olivine aggregates, or enclosed by oikocrysts of orthopyroxene (the xenomorphic texture probably results from reaction replacement of olivine by orthopyroxene). The cumulus olivine exhibits moderate relief, weaker birefringence and is invariably serpentinized; accordingly secondary magnetite is abundant. In contrast, the pegmatitic olivine exhibits higher relief, stronger birefringence, strong undulatory extinction and is essentially fresh and unaltered. Moreover, the pegmatitic olivine always occurs as anhedral grains, even when it is found as fine-grained aggregates intergrown with clinopyroxene. A further distinguishing feature of the pegmatitic olivine is the presence of abundant, orientated, dendrite-like intergrowths of an opaque oxide, which are apparently not found in cumulus olivine in the Bushveld Complex (similar intergrowths were described from olivine in the platinumiferous ultramafic pipes by Wagner, 1929; see also Putnis, 1979).

On the scale of a thin section, locally concordant contact zones between bodies of iron-rich ultramafic pegmatite and harzburgite layers can be seen

to be discordant, usually over a vertical distance of between 1 and 5 cm; pegmatite has partially replaced the harzburgite cumulate. Large grains of pegmatitic olivine and clinopyroxene project into the harzburgite, replacing preferentially the intercumulus phases, first plagioclase and then orthopyroxene. Pegmatitic Fe-Ti oxides and basemetal sulphides do not usually occur in the contact zone. Adjacent to the contact, cumulus olivine grains may be partially resorbed. Further from the contact an initial stage of replacement is preserved in which the 'cumulus' olivine grains are enclosed by a poikilitic, often fine-grained intergrowth of (pegmatite-derived) olivine and clinopyroxene. These latter 'cumulus' olivine grains are hybrids; they retain their primary shape, but are compositionally intermediate between cumulus olivine from unreplaced harzburgite and pegmatitic olivine.

**Mineral chemistry**

Electron microprobe analyses of olivine grains from case studies (1) (sample AD-37A) and (2) (sample AC-A) are presented in Tables 1 and 2. These analyses are of the core zones of discrete grains, although actually no within-grain zonation was detected, possibly because the cumulus olivine grains are so severely serpentinized that only relics can be analysed. In Table 3 average compositions of pegmatitic olivines from the same bodies [sample AD-5, case study (1); sample AC-5, case study (2)], cumulus olivine from the Upper Pseudoreef B (sample A-7/8; Scoon and de Klerk, 1987) and an average pegmatite composition from a number of bodies (that all occur between the UG-2 chromitite layer and the Bastard Reef in the upper Critical Zone) at the Amandelbult Section mine are presented. Electron microprobe data were determined on a Cambridge Microscan unit operating at 20 kV,

TABLE 1 COMPOSITION OF OLIVINE FROM A METASOMATIC CONTACT ZONE

SAMPLE AD-37A													
	1	2	3	4	5	6	7	8	9	10	11	12	13
wt. %													
SiO <sub>2</sub>	35.39	35.51	35.33	37.28	36.53	36.37	36.58	36.77	37.55	37.21	37.74	37.61	38.49
FeO	37.98	38.43	37.39	37.00	37.25	32.39	31.19	29.78	29.51	28.41	22.73	21.93	19.84
MnO	0.47	0.44	0.46	0.45	0.45	0.37	0.37	0.36	0.37	0.37	0.33	0.26	0.25
MgO	25.75	25.41	26.75	26.44	26.68	30.90	31.84	33.09	33.43	33.43	38.82	39.20	39.14
CaO	0.05	0.05	0.04	0.01	0.03	0.03	0.02	0.03	0.03	0.14	0.01	0.04	0.05
NiO	0.08	0.07	0.10	0.10	0.12	0.14	0.21	0.26	0.22	0.24	0.32	0.35	0.31
TOTAL	99.72	99.91	100.07	101.28	101.06	100.20	100.21	100.29	101.11	99.80	99.95	99.39	98.08
cations													
Si	1.0009	1.0038	0.9931	1.0257	1.0113	0.9941	0.9940	0.9917	1.0005	1.0031	0.9874	0.9863	1.0101
Fe <sup>2+</sup>	0.8983	0.9085	0.8790	0.8514	0.8625	0.7404	0.7088	0.6717	0.6576	0.6405	0.4973	0.4810	0.4354
Mn	0.0113	0.0105	0.0110	0.0105	0.0106	0.0086	0.0085	0.0082	0.0084	0.0084	0.0073	0.0058	0.0056
Mg	1.0853	1.0702	1.1203	1.0842	1.1008	1.2588	1.2894	1.3301	1.3275	1.3355	1.5136	1.5321	1.5308
Ca	0.0015	0.0015	0.0012	0.0003	0.0009	0.0009	0.0006	0.0009	0.0009	0.0040	0.0003	0.0011	0.0014
Ni	0.0018	0.0015	0.0022	0.0022	0.0027	0.0031	0.0046	0.0057	0.0047	0.0052	0.0068	0.0074	0.0066
TOTAL	2.9991	2.9960	3.0068	2.9743	2.9888	3.0059	3.0059	3.0083	2.9996	2.9967	3.0127	3.0137	2.9899
mol. % Fo	54.71	54.09	56.04	56.01	56.07	62.96	64.53	66.44	66.87	67.58	75.27	76.11	77.85

TABLE 2 COMPOSITION OF OLIVINE FROM A METASOMATIC CONTACT ZONE

SAMPLE AC-A	1	2	3	4	5	6	7
wt. %							
SiO <sub>2</sub>	37.52	37.44	37.04	36.83	36.59	35.68	35.49
FeO	27.04	26.37	30.91	31.29	31.53	36.27	37.32
MnO	0.33	0.35	0.38	0.35	0.37	0.45	0.47
MgO	34.92	34.17	31.84	31.30	31.07	26.49	26.10
CaO	0.01	0.03	0.01	0.01	0.02	0.02	0.04
NiO	0.30	0.29	0.26	0.23	0.22	0.13	0.17
TOTAL	100.12	98.65	100.44	100.01	99.80	99.04	99.59
cations							
Si	0.9990	1.0090	1.0016	1.0024	1.0000	1.0073	1.0021
Fe <sup>2+</sup>	0.6021	0.5944	0.6990	0.7122	0.7206	0.8564	0.8813
Mn	0.0074	0.0080	0.0087	0.0081	0.0086	0.0108	0.0112
Mg	1.3857	1.3724	1.2831	1.2700	1.2654	1.1146	1.0983
Ca	0.0002	0.0009	0.0003	0.0003	0.0006	0.0006	0.0012
Ni	0.0065	0.0063	0.0060	0.0050	0.0049	0.0030	0.0039
TOTAL	3.0009	2.9910	2.9987	2.9980	3.0001	2.9927	2.9980
mol. % Fo	69.71	69.78	64.73	64.06	63.72	56.55	55.48

using the correction routine of Bence and Albee (1968).

Compositional changes in discrete hybrid grains, expressed as mol. % Fo (at. % Mg/(Mg + Fe<sup>2+</sup>), wt. % NiO and wt. % MnO, across the contact zones in case studies (1) and (2) are illustrated in Figs. 2A, B. Both plots include averages for pegmatitic olivine from the same body; however, the average cumulus composition is plotted only in Fig. 2A, as in case study (2) the sample did not extend to the edge of the (cryptic) contact zone. Evidently the compositional contact does not necessarily coincide with the petrographic contact. From these plots it can be seen that the composition of hybrid olivine in these

contact zones is part-way between that of the primary, cumulus olivine and the pegmatitic olivine. Furthermore, the composition changes in a regular fashion and may be approximated by a straight line.

The composition of pegmatitic olivine grains within the contact zone, e.g. those occurring as fine-grained intergrowths with clinopyroxene that have replaced the original intercumulus phases, is typical of olivine from the core parts of pegmatite bodies. Only the hybrid grains that pseudomorph the cumulus olivine grains exhibit compositional variation.

## Discussion

*Contact zones.* Data presented in Fig. 2 imply that the cumulus olivine grains have re-equilibrated with a (pegmatitic) liquid that had a fixed composition, with respect to the Mg/Fe<sup>2+</sup> ratio and concentration of Ni and Mn. Moreover, data presented by Scoon (1985) suggested that olivine in iron-rich ultramafic pegmatite from a given height in the cumulate pile has a predictable composition (in much the same way as cumulus olivine). Accordingly, it is deduced that the pegmatitic liquid also had a composition related to height in the cumulate pile. The pegmatitic liquid in the upper Critical Zone is Mg-Ni-poor and Fe-rich, as evidenced by whole-rock compositions presented by Viljoen and Scoon (1985). Disequilibrium between cumulus

TABLE 3 AVERAGE COMPOSITION OF OLIVINES

wt. %	AD-5		AC-5		"PEGMATITE"		A-7/8	
	x	s	x	s	x	s	x	s
SiO <sub>2</sub>	34.66 (.1697)		35.16 (.5364)		34.51 (0.4677)		39.63 (.7725)	
FeO	45.05 (.2404)		42.67 (.2404)		44.99 (1.5626)		17.43 (.4333)	
MnO	0.51 (.0071)		0.51 (.0089)		0.56 (0.0364)		0.23 (.0110)	
MgO	20.53 (.1980)		22.03 (.1234)		20.24 (1.3212)		42.55 (.6459)	
CaO	0.08 (.0424)		0.06 (.0100)		0.06 (0.0184)		0.02 (.0104)	
NiO	0.04 (.0071)		0.04 (.0141)		0.044 (0.0174)		0.36 (.0143)	
TOTAL	100.87		100.47		100.40		100.22	
cations								
Si	1.0036		1.0091		-		-	
Fe <sup>2+</sup>	1.0910		1.0244		-		-	
Mn	0.0125		0.0124		-		-	
Mg	0.8859		0.9423		-		-	
Ca	0.0025		0.0018		-		-	
Ni	0.0009		0.0009		-		-	
TOTAL	2.9964		2.9909		-		-	
Fo	44.81 (.3704)		47.92 (.4185)		44.99 (2.47)		81.31 (.2621)	
n <sub>a</sub>	3		5		58		11	
n <sub>s</sub>	1		1		20		2	

AD-5 : Postcumulus olivine, pegmatite body, case study (1)

AC-5 : Postcumulus olivine, pegmatite body, case study (2)

"PEGMATITE" : Average of postcumulus olivine, various pegmatite bodies, upper Critical Zone, Amandelbult Section mine

A-7/8 : Cumulus olivine, Upper Pseudoreef B/C, Amandelbult Section mine

x : mean; s : standard deviation; n<sub>a</sub> : number of analyses; n<sub>s</sub> : number of samples

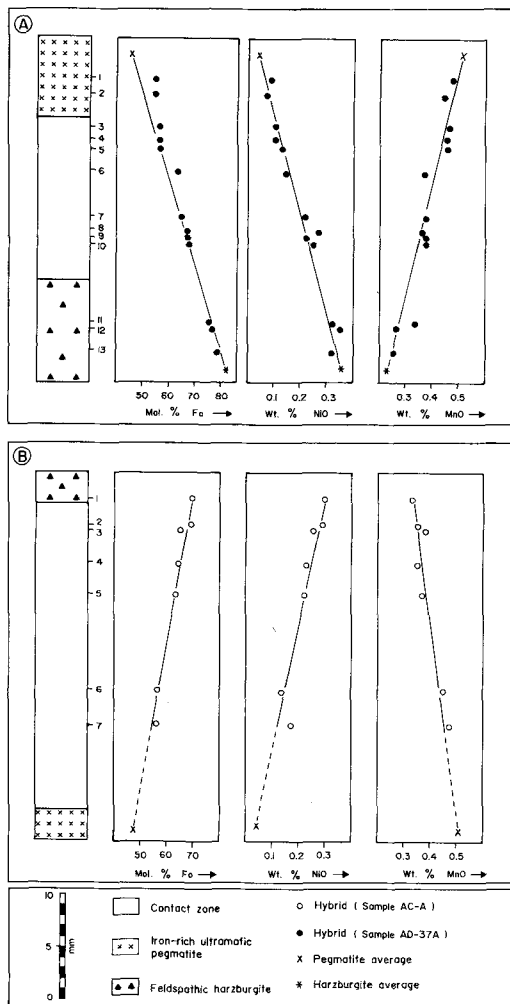


FIG. 2. Vertical profiles, on the scale of one or two thin sections, through samples AD-37A (A) and AC-A (B). Sample numbers refer to analyses in Tables 1 and 2. Average pegmatite compositions are samples AD-5 (A) and AC-5 (B); the average harzburgite composition in (A) is sample A-7/8 (Table 3).

olivine crystals and pegmatitic liquid thus resulted in cation-for-cation exchange of Mg, Ni and Si for Fe<sup>2+</sup> and Mn. Excess Mg, Ni and Si, it is assumed, are flushed from the system. I suggest that different exposure times, a function of the extent to which the pegmatitic liquid infiltrated the harzburgite layer, resulted in the straight line relationships. This process may be designated 'magmatic metasomatism', as described by Korzhinsky (1965).

*Nickel.* On a plot of wt.% NiO against wt.%

MgO these data approximate to two straight lines (Fig. 3):

$$\text{Case study (1): MgO} = (53.59 \times \text{NiO}) + 20.77 \quad (n_d = 14; cc = 0.958) \quad (1)$$

$$\text{Case study (2): MgO} = (49.56 \times \text{NiO}) + 19.58 \quad (n_d = 8; cc = 0.981) \quad (2)$$

where MgO and NiO are in wt.%,  $n_d$  is the number of data points and  $cc$  is the correlation coefficient. Equation (1) embraces analyses from samples AD-37A ( $n_d = 13$ ) and AD-5 ( $n_d = 1$ ), and equation (2) includes analyses from samples AC-A ( $n_d = 7$ ) and AC-5 ( $n_d = 1$ ). These linear regressions exclude the average cumulus composition as the hybrid olivines exhibit unusually high NiO/MgO ratios. These data imply that metasomatism of Mg-Ni-rich olivine by an iron-rich liquid results in more

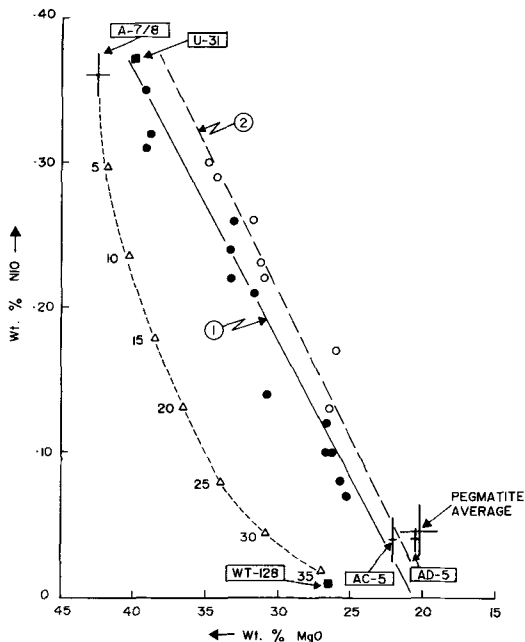


FIG. 3. Plot of wt.% NiO against wt.% MgO in olivine. Solid symbols are from sample AD-37A, open symbols are from sample AC-A. For linear regressions see equations (1) and (2) in text. Average compositions are plotted as error bars which represent plus-minus one standard deviation from the mean (Table 3). Dashed line represents a theoretical fractional crystallization curve (plotted at crystallization intervals of 5%) calculated assuming the initial liquid is in equilibrium with sample A-7/8 (for explanation see Irvine, 1980; Scoon and de Klerk, 1987). The liquid is depleted in Ni after 35% crystallized. For explanation of samples U-31 and WT-128 see text (Ni was below the lower limit of determination (0.01 wt.% NiO) in sample WT-128).

efficient exchange of Mg than Ni. The resulting 'metasomatic trend', which might be expected to give a straight line connecting the end-member cumulus and postcumulus compositions, is thus offset at the cumulus-end (Fig. 3).

These metasomatic trends are distinct from theoretically generated olivine fractionation curves (one such plot shown in Fig. 3), as olivine which is fractionally crystallized from a tholeiitic magma is rapidly depleted in Ni. Unfortunately, the theoretical fractionation paths cannot be verified against measured values as cumulus olivine within the compositional range  $Fo_{77}$  (sample U-31, UG-2 cyclic unit, upper Critical Zone; Scoon and de Klerk, 1987) to  $Fo_{56}$  (sample WT-128, from 8 m

below the main magnetite layer, Upper Zone; Scoon, 1985) is absent in the Bushveld Complex (the 'olivine gap' was described from the Bushveld Complex by Wager and Brown, 1968). However, it is significant that the first cumulus (iron-rich) olivine to crystallize after the olivine gap ( $Fo_{56}$  according to Scoon, 1985;  $Fo_{49}$  according to Wager and Brown, 1968) is nickel-poor ( $NiO < 0.01$  wt.%). Even if it is assumed that within the olivine gap in the Bushveld Complex, olivines do not follow a theoretical fractionation path, the most Ni-rich 'cumulus trend' possible is a straight line between samples U-31 or A-7/8 and sample Wt-128 (Fig. 3). As  $D^{Ni}(\text{oliv/liq}) \gg D^{MgO}(\text{oliv/liq})$  the cumulus trend would most likely lie closer to the Ni-axis.

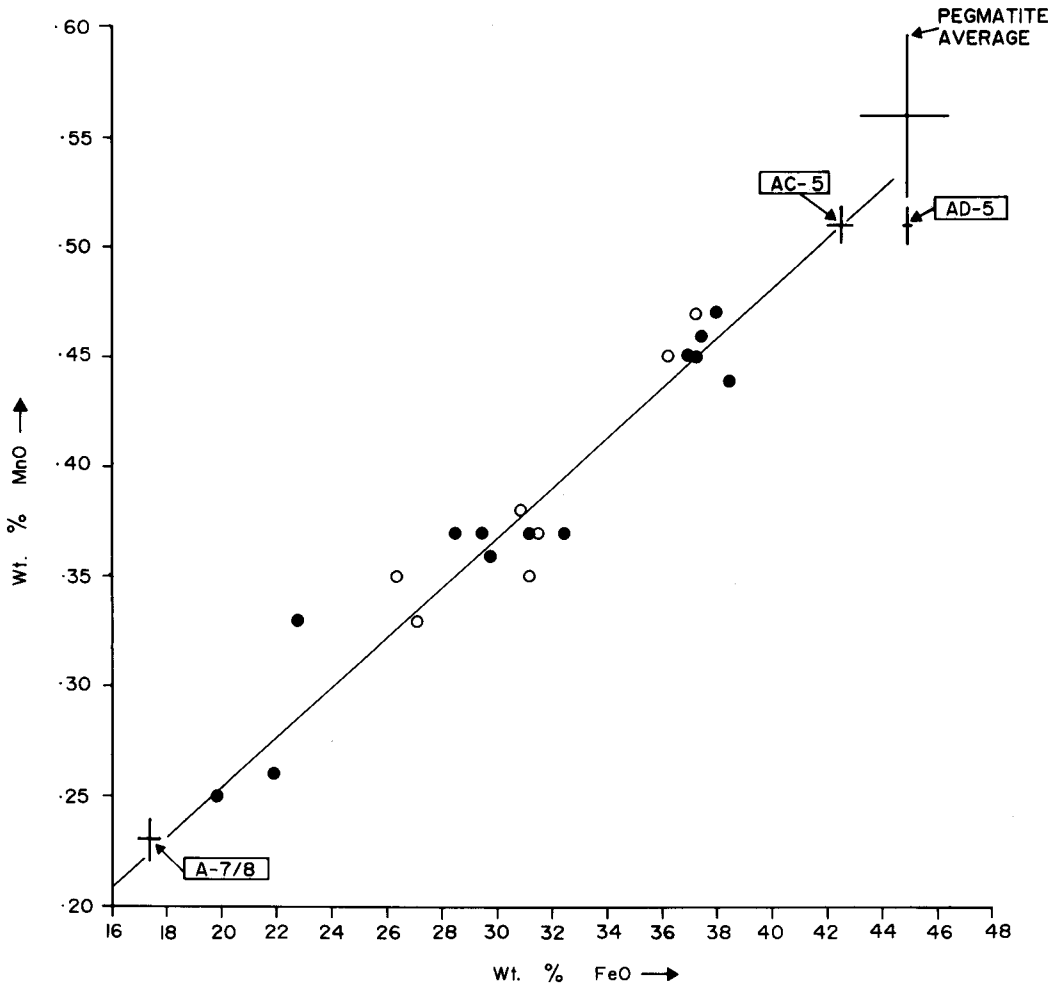


FIG. 4. Plot of wt.% MnO against wt.% FeO in olivine. Solid symbols are from sample AD-37A, open symbols are from sample AC-A. For linear regression see equation (3) in text.

Accordingly, I suggest that metasomatic olivine may be distinguished from cumulus olivine in the Bushveld Complex by a plot of NiO against MgO.

Olivines with unusually high NiO/MgO ratios have been reported from the Muscox intrusion by Irvine (1980). Compositional breaks between cyclic units in the Muscox layered sequence are defined by the  $Mg/(Mg + Fe^{2+})$  ratio and the Ni content of olivine; however, 'in each case the difference for the  $Mg/Fe^{2+}$  discontinuity is 2-4 times larger than that for the Ni discontinuity' (Irvine, 1980, p. 341). Irvine explains these features by a process of 'magmatic infiltration metasomatism' in which the cumulus olivine grains are exposed to upward-migrating intercumulus silicate liquid. Differences between the  $Mg/Fe^{2+}$  and Ni discontinuities are attributed to the composition of the intercumulus (Mg-Ni-poor, Fe-rich) liquid which contains about one third as much  $(Mg + Fe^{2+})$  as the crystals but only about one tenth as much Ni; thus the adjustment to obtain equilibrium between the Ni content of the liquid and the crystals is relatively small (Irvine, 1980, p. 353). A similar argument may be used to explain the data in this study, as the metasomatizing liquid, it is proposed, also has a relatively high  $(Mg + Fe^{2+})$  content and low Ni content (see Viljoen and Scoon, 1985).

**Manganese.** On a plot of wt.% MnO against wt.% FeO these data define a single straight line (Fig. 4):

$$FeO = (88.60 \times MnO) - 2.56 \\ (n_s = 23; cc = 0.974) \quad (3)$$

calculated from samples AD-37A ( $n_d = 13$ ), AC-A ( $n_d = 7$ ), AD-5 ( $n_d = 1$ ), AC-5 ( $n_d = 1$ ) and the average cumulus composition, sample A-7/8 ( $n_d = 1$ ). These data regress back to the primary (average) cumulus composition, implying that metasomatic addition of  $Fe^{2+}$  and Mn, under these conditions, reflects a constant  $D^{Fe/Mn}(oliv/liq)$ . Note also that iron-rich ultramafic pegmatite (and presumably the pegmatitic liquid) has a higher Mn content than the cumulus olivine crystals, so that metasomatic exchange of Mn does not mirror that of Ni.

**Metasomatic olivine.** The distinction between metasomatic olivine and igneous olivine that has fractionally crystallized from a magma is significant because the role of metasomatism in layered intrusions is receiving increasing attention. Moreover, numerous publications have attributed the formation of discordant bodies of ultramafic rock in layered complexes to metasomatism. The metasomatic process documented in this study resulted from reaction between cumulus crystals and silicate liquid i.e. magmatic metasomatism. These data cannot be reconciled with a low-temperature

aqueous metasomatic model based on the experimental study of Bowen and Tuttle (1949), such as that proposed by Cameron and Desborough (1964).

Postcumulus, ultramafic rocks in the Bushveld Complex can be subdivided on the basis of olivine composition into two groups: iron-rich and magnesium-rich e.g. groups (1) and (2), respectively, in the classification of Viljoen and Scoon (1985). The third group, i.e. the platiniferous ultramafic pipes, consists of both iron- and magnesium-rich olivines. Significantly, the chemical trends presented in this paper are duplicated by iron-rich olivines in the platiniferous ultramafic pipes (Scoon, 1985). Therefore, I suggest that iron-rich olivine in these pipes also formed by magmatic metasomatism of pre-existing magnesian olivine. However, I have not found any chemical evidence to support the formation of magnesian olivine in discordant bodies in the Bushveld Complex by metasomatism (this problem will be discussed more fully in a separate paper dealing with the platiniferous ultramafic pipes).

The recognition of these metasomatic trends thus has considerable importance in the interpretation of discordant bodies of ultramafic rock in layered complexes. However, the metasomatic olivines described here all formed by the replacement of pre-existing cumulus olivine and no chemical evidence has been found to support the formation of olivine in iron-rich ultramafic pegmatite by metasomatism of other phases. Finally, these data may argue against a metasomatic origin for magnesian olivine in postcumulus, ultramafic rocks, as reaction between cumulus crystals and intercumulus liquid would surely result in more fractionated olivine compositions as documented by Irvine (1980) and this study.

#### Acknowledgement

I thank Prof. H. V. Eales for improving an earlier draft of this manuscript.

#### References

- Bence, A. E., and Albee, A. L. (1968) *J. Geol.* **76**, 382-403.
- Bowen, N. L., and Tuttle, O. F. (1949) *Bull. Geol. Soc. Am.* **50**, 439-60.
- Cameron, E. N., and Desborough, G. A. (1964) *Econ. Geol.* **59**, 197-225.
- and Glover, E. D. (1973) *Am. Mineral.* **58**, 172-88.
- Irvine, T. N. (1980) In *Physics of magmatic processes* (R. B. Hargreaves, ed.), 325-83.
- Korzhiinsky, D. S. (1965) *Am. J. Sci.* **263**, 193-205.

- Putnis, A. (1979) *Mineral. Mag.* **43**, 293–6.
- Scoon, R. N. (1985) Unpubl. Ph.D. thesis, Rhodes University, Grahamstown, South Africa.
- and de Klerk, W. J. (1987) *Can. Mineral.* **25**, 51–77.
- Viljoen, M. J., and Scoon, R. N. (1985) *Econ. Geol.* **80**, 1109–28.
- Theron, J. C., Underwood, B., Walters, B. M., Weaver, J., and Peyerl, W. (1986) In *Mineral Deposits of Southern Africa* (Anhaeusser, C., and Maske, S., eds.), 1041–60.
- Wager, L. R., and Brown, G. M. (1968) *Layered igneous rocks*, Oliver and Boyd, 588 pp.
- Wagner, P. A. (1929) *The platinum mines and deposits of South Africa*, Oliver and Boyd, 326 pp.

[Manuscript received 6 August 1986;  
revised 3 November 1986]